PROCEEDINGS OF SCIENCE

Performance of ATLAS RPC detectors and L1 Muon Barrel Trigger with a new CO_2-based gas mixture

Eric Ballabene [a,b,*]
on behalf of the ATLAS Collaboration

[a] *Department of Physics and Astronomy A. Righi, University of Bologna, Viale Carlo Berti Pichat, 6/2, Bologna, Italy*
[b] *INFN, Sezione di Bologna, Viale Carlo Berti Pichat, 6/2, Bologna, Italy*

E-mail: eric.ballabene@cern.ch

Resistive Plate Chambers are used in the ATLAS experiment for triggering muons in the barrel region. These detectors use a Freon-based gas mixture containing $C_2H_2F_4$ and SF_6, high global warming potential greenhouse gases. To reduce the greenhouse gas emissions and cost, it is crucial to search for new environmentally friendly gas mixtures. In August 2023, at the end of the proton-proton data-taking campaign, ATLAS collaboration decided to replace the standard gas mixture (94.7% $C_2H_2F_4$, 5.0% i-C_4H_{10}, 0.3% SF_6) with a new CO_2-based gas mixture: 64% $C_2H_2F_4$, 30% CO_2, 5.0% i-C_4H_{10}, 1% SF_6. The performance of the RPC detectors with the new gas mixture is presented with a particular emphasis on detector efficiency, cluster size and timing performance, as well as the efficiency of the L1 Muon Barrel trigger system.

42nd International Conference on High Energy Physics (ICHEP2024)
18-24 July 2024
Prague, Czech Republic

*Speaker

PoS(ICHEP2024)872

1. The ATLAS RPC detector

The ATLAS [1, 2] Resistive Plate Chamber (RPC) detectors [3, 4] can be regarded as a large planar capacitor with two parallel high resistivity electrodes ($\sim 10^{10}$ Ωcm) both externally coated by a graphite layer, separated by insulating spacers, defining a gas gap of 2 mm. The gap is filled with a suitable gas mixture at atmospheric pressure representing the target for the ionizing radiation.

Each RPC singlet comprises two readout panels, which are placed on the outer faces of the electrodes. The readout panels are made with $\eta-$ or $\phi-$oriented strips and they are equipped with Front-End (FE) electronics at opposite strip ends. A schematic drawing of an ATLAS RPC detector module is shown in Figure 1 (left).

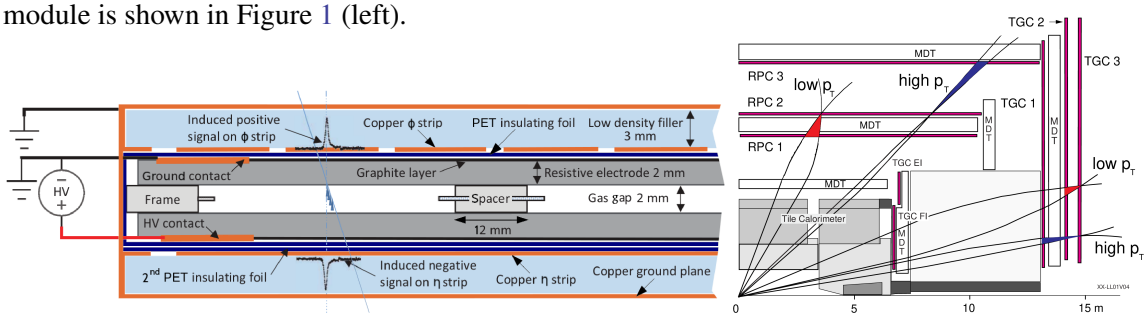

Figure 1: A schematic drawing of an ATLAS RPC detector module (left). Illustration of the low-p_{T} and high-p_{T} L1 muon trigger algorithms in the barrel and endcap regions (right).

The RPC chambers are made of two independent detector layers and are arranged in 3 concentric cylindrical shells of which two are on the opposite sides of the Barrel Middle (BM) layer of MDT chambers and one is on the innermost side of the Barrel Outer (BO) MDT layer. They are operated in a toroidal magnetic field of about 0.5 T.

The RPC system provides the Level 1 (L1) hardware muon trigger in the barrel [5]. Two types of muon triggers are implemented and indicated in Figure 1 (right): low-p_{T} triggers, which require a coincidence between two layers in BM, and high-p_{T} triggers, which require a coincidence between a BM pivot layer and a BO layer. The barrel trigger system is sub-divided into 432 projective towers, each provided with on-detector trigger and readout electronics boards containing the processor boxes (PADs) for low- and high-p_{T} triggers. The hit coincidences are implemented by custom Coincidence Matrix ASICs (CMAs) in the PAD boxes. The CMAs align the FE signals in time, check the time coincidence of RPC hits and perform trigger logic operations.

2. The RPC detector in Run 3

After a successful data taking period in Run 2, the detector has undergone an intense maintenance to ensure an efficient data taking during Run 3. Several interventions have been carried out on the detector, mainly covering the gas distribution with the aim of stabilizing the system and reducing the amount of gas released in the atmosphere: installation of non-return valves on the chamber outputs to avoid reverse flow with large leaks, a massive gas leak repair campaign to fix the continuously developing leaks, a new technique to repair and prevent new leaks and the installation of additional gas distribution racks to increase the vertical segmentation of the current RPC detectors and in view of the installation of new Phase-II chambers. In addition, the segmentation

for the HV channels has been doubled in a third of the spectrometer to mitigate the effect of detector failures and the gas mixture has been changed adding a CO_2 gas fraction.

In particular, during 2022 and 2023 in Run 3, the RPCs were continuously flushed with a gas mixture composed of $C_2H_2F_4$ (the gas target for the primary ionization), i-C_4H_{10} (a quencher component that helps to avoid propagation of the discharge) and SF_6 (an electronegative component that helps to limit the growth of avalanches). The $C_2H_2F_4$ gas has a strong greenhouse effect and it is currently being phased down in the European Union, thereby also leading to rising cost.

The RPC gas mixture was changed during Run 3 in August 2023 from $C_2H_2F_4$ (94.7%), i-C_4H_{10} (5%) and SF_6 (0.3%) to $C_2H_2F_4$ (64%), CO_2 (30%), i-C_4H_{10} (5%) and SF_6 (1%). The Global Warming Potential (GWP), which measures how much infrared thermal radiation a greenhouse gas would absorb over a given time, is the following for each component: 1430 for $C_2H_2F_4$, 3.3 for C_4H_{10}, 22800 for SF_6 and 1 for CO_2. The new gas mixture yields a $\sim$ 14% reduction of the GWP.

Due to the different properties of the new gas mixure, the operational High Voltage (HV) applied to the RPC chambers had to be changed. The reference voltage applied across all detector chambers was 9.6 kV before the gas mixture change, while the new applied voltage is 9.35 kV. The reference operational voltage V_{ref} is corrected for local changes in environmental pressure p and temperature T at chamber level with respect to the reference conditions by the HV correction factor $\rho(p,T)$. The applied operational voltage V_{app} is therefore given by [6]

$$V_{\text{app}} = V_{\text{ref}}\,\rho(p,T) \tag{1}$$

where

$$\rho(p,T) = \left[1+\alpha_p\left(\frac{p}{p_0}-1\right)\right]\left[1+\alpha_T\left(\frac{T_0-273.15}{T-273.15}-1\right)\right]. \tag{2}$$

In the formula, $\alpha_p = 0.8$, $\alpha_T = 0.5$, $p_0 = 9.6\cdot 10^4$ Pa, $T_0 = 294.15$ K, $V_{\text{ref}} = 9350$ V and $0.98 \le \rho(p,T) \le 1.02$. During May 2024, the HV correction factor $\rho(p,T)$ was updated to take into account a new pressure probe (replacing an old probe suffering of miscalibration problems) and local changes of pressure and temperature for the BO chambers whose segmentation for the HV channels has been doubled. The updated HV correction factor led to an increase between ~30 V and ~150 V for some of the RPC chambers, resulting in an increase of the mean gas gap current and improving the stability of the RPC trigger efficiency.

3. Performance of the RPC detector

The first effect observed with the new gas mixture is an increase of the gas gap currents. Figure 2 (left) shows the distributions of the measured current density for all the RPC gas gaps at the instantaneous luminosity of $2.0\times10^{32}\,\text{cm}^{-2}\text{s}^{-1}$ for 3 different ATLAS Runs. The addition of the CO_2 leads to an increase of the current density of the gas gaps of around $\sim$ 17% in agreement with prototype results [7], even if the operational voltage has been lowered with the new gas mixture. The gas gap current density is also shown as a function of the instantaneous luminosity in Figure 2 (right), where a linear increase of the RPC mean gap current density as a function of the instantaneous luminosity is found.

Another key detector information is the cluster size. In principle, the addition of the CO_2 component in the gas mixture would increase the cluster size but the increased SF_6 fraction in the

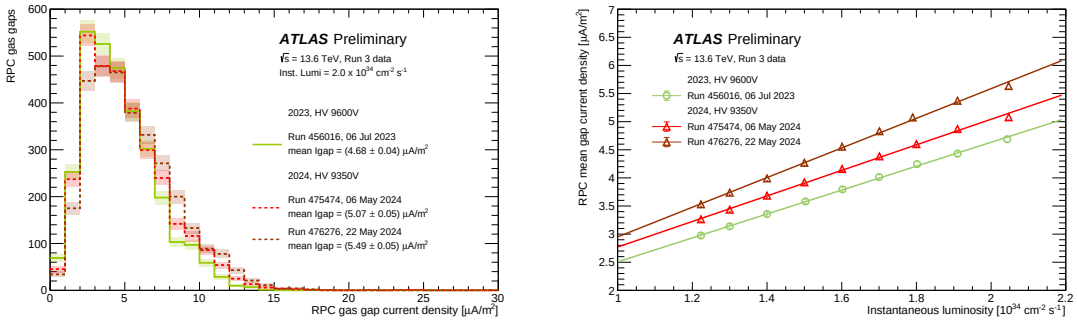

Figure 2: Measured RPC gas gap current density at the instantaneous luminosity of 2.0×10^{32} cm^{-2}s^{-1} (left) and as a function of the instantaneous luminosity (right) for three ATLAS Runs: Run 456016 in 2023 before the gas mixture change, Run 475474 in 2024 after the gas mixture change but before the HV correction factor update and Run 476276 in 2024 after the gas mixture change and after the HV correction factor update.

gas mixture would limit the dimension of the avalanche. Figure 3 shows the cluster size for a Run in 2023 (left) and for a Run in 2024 (right). The measured mean cluster size is 1.42 in the η view

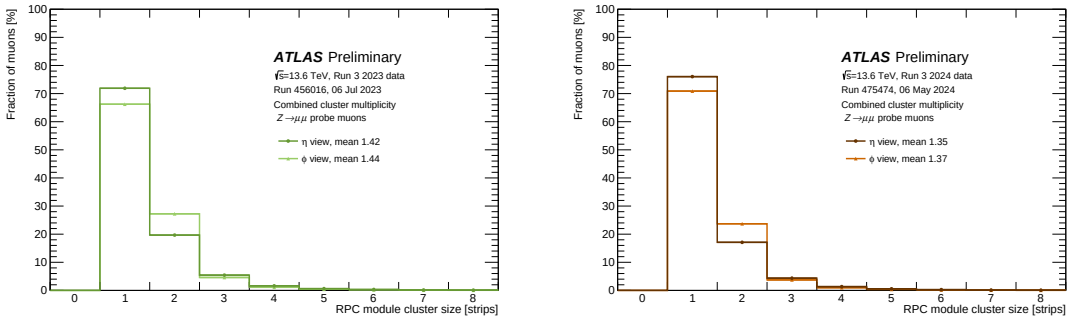

Figure 3: Cluster size distributions for Run 456016 in 2023 (left) and for Run 475474 in 2024 (right).

and 1.44 in the ϕ view for the Run in 2023, while it is 1.35 in the η view and 1.37 in the ϕ view for the Run in 2024. Therefore, a similar cluster size is measured between 2023 and 2024 years, slightly smaller in 2024 than in 2023. The fact that the cluster size did not increase in 2024 also implies that there are no signs of detector ageing effects yet.

4. Performance of the RPC L1 trigger

The RPC trigger efficiency was monitored throughout the ATLAS Run 3 data taking. Figure 4 shows the L1 muon barrel trigger efficiency (result of the convolution of the detector efficiency with its geometrical acceptance) for the ATLAS Runs in 2023 (left) and in 2024 (right) as a function of the Run Number, measured on events selected with non-muon triggers. The L1 muon barrel trigger efficiency is found to be overall fairly constant during 2023 and 2024 years although fluctuating from run to run. Some instabilities at the beginning of 2024 were fixed by the updated version for handling the HV correction factor $\rho(p,T)$.

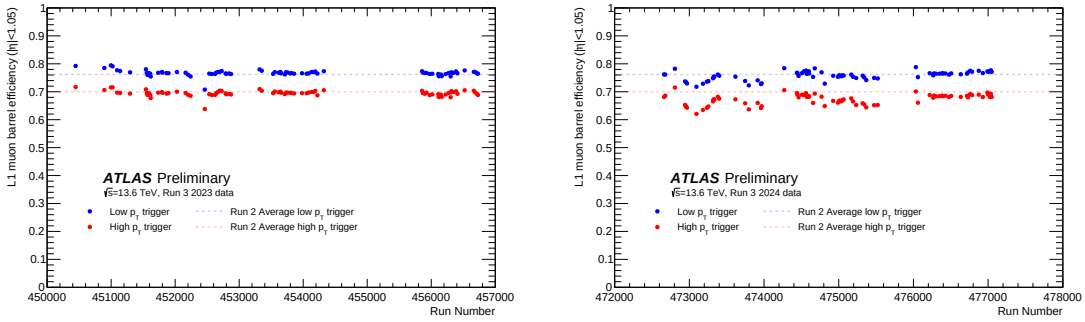

Figure 4: L1 muon barrel trigger efficiency for 2023 (left) and 2024 (right) as a function of the Run Number, obtained with non-muon triggers on the physics main-stream.

The RPC trigger efficiency is also shown as a function of the offline muon p_{T} for different L1 trigger thresholds in Figure 5, for a Run in 2023 (left) and for a Run in 2024 (right). Constant RPC trigger performance is observed between 2023 and 2024 for the different L1 trigger thresholds.

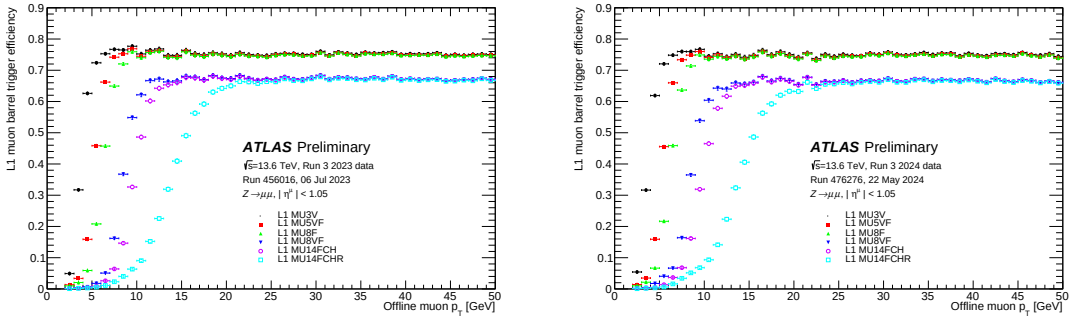

Figure 5: L1 muon barrel trigger efficiency as a function of the offline muon p_{T} for Run 456016 in 2023 (left) and for Run 476276 in 2024 (right) for different L1 triggers used in Run 3.

Finally, the L1 muon barrel trigger efficiency is studied as a function of the offline muon η and ϕ, separately for the high-p_{T} and low-p_{T} triggers. Figure 6 shows the high-p_{T} RPC trigger efficiency while Figure 7 shows the low-p_{T} trigger efficiency, both for a Run in 2023 (left) and for a Run in 2024 (right). Constant trigger performance between 2023 and 2024 is found for both high-p_{T} and low-p_{T} triggers. Improvements in specific regions of the 2024 η-ϕ maps are due to the extensive 2023 Year-End Technical Stop (YETS) interventions.

5. Conclusions

The ATLAS RPC detector is operating with a new gas mixture since August 2023. The gas mixture was changed during Run 3 at the end of the 2023 pp collisions. The RPC detector and trigger performance before and after the new gas mixture is being monitored and studied. The new gas mixture at detector level is behaving as expected, yielding an increase of ~17% in the gas gap current and a similar cluster size. The measured trigger efficiency during 2024 is at a similar level to 2023. The RPC operations during Run 3 are progressing successfully with the focus on reducing gas leaks and increasing as much as possible the trigger coverage.

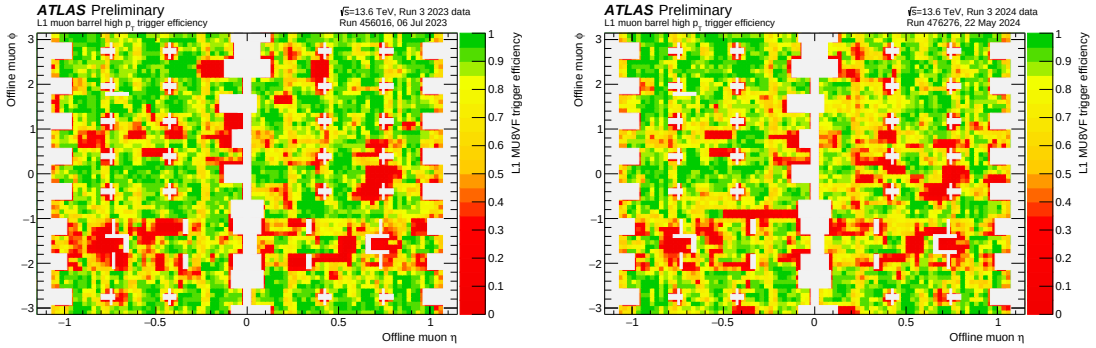

Figure 6: High-p_{T} L1 muon barrel trigger efficiency as a function of the offline muon η and ϕ for Run 456016 in 2023 (left) and for Run 476276 in 2024 (right).

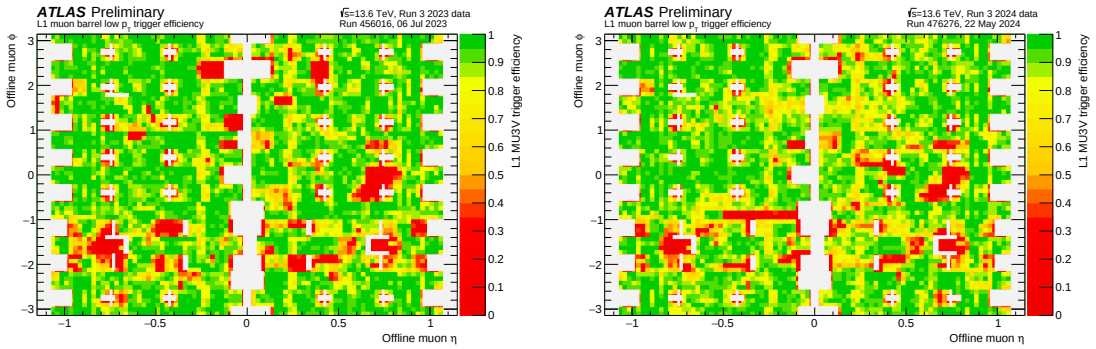

Figure 7: Low-p_{T} L1 muon barrel trigger efficiency as a function of the offline muon η and ϕ for Run 456016 in 2023 (left) and for Run 476276 in 2024 (right).

References

[1] The ATLAS Collaboration, *The ATLAS Experiment at the CERN Large Hadron Collider*, *JINST* **3** (2008) S08003.

[2] The ATLAS Collaboration, *The ATLAS Experiment at the CERN Large Hadron Collider: A Description of the Detector Configuration for Run 3*, *JINST* **19** (2024) P05063.

[3] R. Santonico and R. Cardarelli, *Development of resistive plate counters*, *Nucl. Instrum. and Meth.* **187** (1981).

[4] R. Cardarelli et al., *Progress in resistive plate counters*, *Nucl. Instrum. and Meth.* **263** (1988).

[5] F. Anulli et al., *The Level-1 Trigger Muon Barrel System of the ATLAS experiment at CERN*, *JINST* **4** (2009) P04010.

[6] G. Aielli et al., *Performance, operation and detector studies with the ATLAS Resistive Plate Chambers*, *JINST* **8** (2013) P02020.

[7] G. Rigoletti et al., *Performance studies of RPC detectors operated with $C_2H_2F_4$ and CO_2 gas mixtures*, *Nucl. Instrum. and Meth.* **1049** (2023).